Delft University of Technology

Flow around a pair of 2D cylinders using a hybrid Eulerian-Lagrangian solver

Pasolari, R.; Ferreira, Carlos; van Zuijlen, A.H.

Important note
To cite this publication, please use the final published version (if applicable).
Please check the document version above.

PAPER • OPEN ACCESS

Flow around a pair of 2D cylinders using a hybrid Eulerian-Lagrangian solver

To cite this article: R. Pasolari *et al* 2024 *J. Phys.: Conf. Ser.* **2767** 052006

View the article online for updates and enhancements.

Flow around a pair of 2D cylinders using a hybrid Eulerian-Lagrangian solver

R.Pasolari, C. Ferreira and A. van Zuijlen

Faculty of Aerospace Engineering, Delft University of Technology, Delft, The Netherlands

E-mail: `r.pasolari@tudelft.nl`

Abstract. The field of external aerodynamics encompasses various engineering disciplines with a significant impact on wind energy technology. Aerodynamic investigations provide insights not only into the characteristics of individual blades or standalone wind turbines but also into entire wind farms. As advancements in wind turbine design continue, understanding the interactions between turbines in close proximity becomes crucial, presenting a multi-body problem. Researchers require efficient and accurate tools to comprehensively study such dynamics. This paper presents a hybrid Eulerian-Lagrangian solver designed to leverage the strengths of Eulerian solvers in resolving boundary layers and Lagrangian solvers in convecting wakes downstream without introducing significant numerical diffusion. The solver adeptly handles multi-body simulations, allowing the construction of independent Eulerian meshes that communicate seamlessly through Lagrangian particles. In this way, the computational study of multibody problems does not require very large and dense meshes. Validation in single-body cases has already been conducted, with this paper demonstrating the solver's application to a pair of cylinders in different configurations. A comparative performance analysis is carried out against pure Eulerian solvers. The results highlight that the hybrid solver efficiently reproduces the accuracy of the Eulerian solver, demonstrating its effectiveness in handling complex aerodynamic simulations.

1. Introduction

Researchers are dedicated to identifying strategies that enhance the efficiency of wind farms and amplify power output without substantially expanding the physical footprint of these farms. It is evident that a comprehensive understanding of wind energy necessitates moving beyond the examination of individual blades or standalone turbines. Wind turbines are integral components of a larger system—the wind farm. The interaction between turbines within the wind farm results in a significant change in the airflow dynamics as compared to a standalone wind turbine. As a result, understanding a wind farm's dynamics falls within the domain of multibody problems. It is crucial for researchers to come up with efficient but also accurate methodologies to study such problems.

Aerodynamic problems can typically be studied experimentally and numerically. However, in the context of multibody problems, experiments can be prohibitively expensive in terms of both time and money, so often, numerical simulations are preferred. In numerical simulations, the Eulerian approach is often employed, such as Finite Volumes and Finite Elements, and the solid bodies can be fully resolved [1], or they can be modeled as actuator disks [2], to reduce the computational cost. On the other hand, Lagrangian methods are often used, like the Vortex

Particle Methods (VPM), which offer accelerated solutions, often sacrificing the boundary later resolution. Finally, the Blade Element Method (BEM) is a commonly used low-fidelity method that provides fast results in wind turbine simulations [4].

In the past two decades, a numerical approach gaining increasing attention—and the focus of this paper—is the coupled Eulerian-Lagrangian method. This approach seeks to harness the strengths of both Eulerian and Lagrangian solvers to create a tool capable of accurately resolving boundary layers (via the Eulerian solver) and efficiently evolving the wake downstream without introducing numerical diffusion. Numerous research groups have contributed to the development of hybrid methods in recent years [5, 6, 7, 8]. Pasolari et al. [5] coupled OpenFOAM with a VPM for conducting 2D simulations, Billuart et al. [6] developed a weak coupling approach between a body-fitted velocity-pressure solver and a Vortex Particle-Mesh method in two dimensions, Papadakis et al. [7] integrated a compressible Eulerian solver (MaPFlow) with a Lagrangian solver using a Vortex Particle-Mesh technique and Stock et al. [8] coupled a high-order spectral finite difference method with an open-source VPM. The specific methodology addressed in this paper corresponds to the hybrid solver developed by Pasolari et al. [5]. In that paper, the authors showcase the demonstration and validation of this hybrid solver. Validation is performed using a 2D flow around a sole cylinder case at low Reynolds numbers (Re = 550). This serves as a robust validation scenario for the hybrid solver's capabilities.

A great advantage of the hybrid solver is its efficient way on handling multibody problems. It allows for the creation of very narrow Eulerian meshes for each body independently, with the Lagrangian solver serving to interconnect them. This approach proves to be not only highly practical but also elegant in its treatment of multibody simulations. A more detailed explanation of this methodology will be provided in the next section, and for a deeper understanding, readers are encouraged to refer to the reference paper [5].

In the specific context of this paper, the hybrid solver is extended to simulate multibody problems. The methodologies employed for this extension are thoroughly presented, followed by a comprehensive validation process. Validation is carried out through various scenarios involving the 2D flow around a pair of cylinders. These cylinders are arranged in two different configurations to assess the solver's robustness. Firstly, the two cylinders are positioned in a tandem arrangement with two cases to be tested: one where the two cylinders are positioned very close ($L = 1.5D$), where L is the horizontal distance of their centers, and D is the diameter of the cylinder; and one where they are further apart ($L = 3.0D$). Then, the two cylinders are positioned in a staggered arrangement (one on top of the other). Similarly, two cases are tested: one where their distance is close ($T = 1.5D$), where T is the vertical distance of the centers of the cylinders, and one where they are further apart ($T = 3.0D$). In both cases above, the scenario where the cylinders are very close tests the most extreme case where the two meshes overlap in a very large part and serves as validation for the solver's ability to handle such extreme scenarios. All the hybrid run for $Re = 200$ and the results are compared with the corresponding results obtained from pure Eulerian simulations.

2. The hybrid solver

The hybrid solver strategically leverages the strengths and mitigates the weaknesses of both Eulerian and Lagrangian solvers, which complement each other in a synergistic manner. Specifically, Eulerian solvers excel at resolving flows near solid surfaces without requiring a vast number of elements, thanks to the introduction of anisotropic elements. However, they introduce significant artificial diffusion, making them less efficient in resolving the far-field region. On the other hand, Lagrangian solvers, and more specifically VPM that is used here, cannot capture phenomena occurring close to the body but can efficiently evolve the solution in regions where convective terms dominate.

The foundation of the specific hybrid solver lies in the Domain Decomposition method,

initially proposed by Daeninck [9], later refined by Stock et al. [8], and successfully applied in Palha et al. [10]. The fluid domain is decomposed as illustrated in Figure 1. The Eulerian solver resolves the region in proximity to the solid boundary to capture vorticity generation and viscous phenomena on the solid surface, while the Lagrangian solver is responsible for evolving the wake downstream. This approach ensures that the advantages of each solver can be fully exploited.
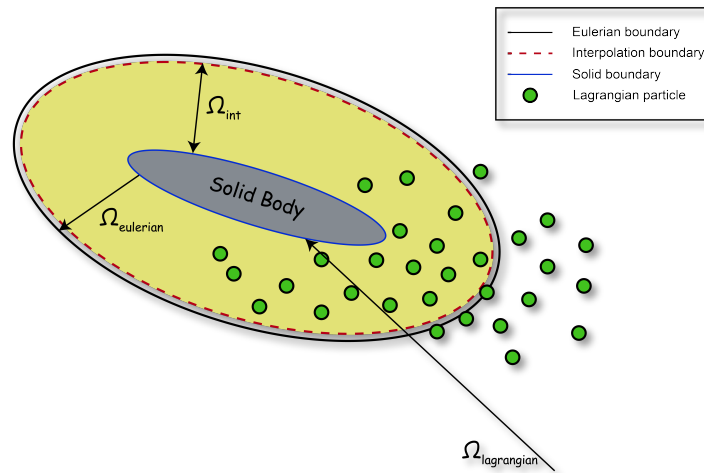

Figure 1: The decomposition method used in the hybrid Eulerian-Lagrangian solver.

2.1. The Eulerian solver

In the hybrid framework of this project, the Eulerian component relies on OpenFOAM v9 [11]. OpenFOAM, being open-source, provides the flexibility to implement new solvers and modify existing ones, making it widely embraced in both research and academia. Specifically, the pimpleFOAM solver within OpenFOAM is employed for the hybrid solver presented in this project. PimpleFOAM is an intrinsic OpenFOAM solver designed to address transient, incompressible laminar, and turbulent flows. Notably, it employs the PIMPLE loop to facilitate the coupling of the velocity and pressure fields, ensuring the mass conservation.

2.2. The Lagrangian solver

In the Lagrangian part of the hybrid solver, the Vortex Particle Method (VPM) is utilized. VPM operates by assigning Lagrangian particles to carry the vorticity of the flow—an essential quantity closely connected to the aerodynamic forces exerted on the studied body. This characteristic makes VPMs highly favored in the field of external aerodynamics.

In the equations presented in this section, the following symbols are used:

$$u : \text{velocity field,}$$
$$\omega : \text{vorticity field,}$$
$$\boldsymbol{x} : \text{position,}$$
$$\Gamma : \text{circulation,}$$
$$r : \text{distance,}$$
$$\sigma : \text{core radius,}$$
$$\boldsymbol{e_z} : \text{unit vector in the z-direction.}$$

Additionally, the subscripts p and ∞ correspond to the particle and freestream conditions, respectively.

VPM relies on the vorticity-velocity formulation of the Navier-Stokes (N-S) equations, as illustrated in Eq. 1:

$$\frac{\partial \boldsymbol{\omega}}{\partial t} + (\boldsymbol{u} \cdot \boldsymbol{\nabla}) \boldsymbol{\omega} = (\boldsymbol{\omega} \cdot \boldsymbol{\nabla}) \boldsymbol{u} + \nu \nabla^2 \boldsymbol{\omega} \qquad \text{in 3D} \qquad (1a)$$

$$\frac{\partial \omega}{\partial t} + (\boldsymbol{u} \cdot \boldsymbol{\nabla}) \omega = \nu \nabla^2 \omega \qquad \text{in 2D} \qquad (1b)$$

In two-dimensional flows, the vortex stretching term is zero and so it can dropped off the equations, while the vorticity has only one non-zero component, rendering it a scalar. To discretize the flow field, vortex particles are employed, and frequently, a finite core is attributed to the initially singular particles. This practice aims to mitigate the occurrence of spiky solutions that can arise from the use of Dirac's functions. The induced velocity and vorticity fields are computed as the summation of the induced fields by each particle, expressed as shown in Eq. 2:

$$\boldsymbol{u}_p(\boldsymbol{x}) = -\frac{1}{2\pi} \sum_p \frac{g_\sigma(|\boldsymbol{x} - \boldsymbol{x_p}|)}{|\boldsymbol{x} - \boldsymbol{x_p}|^2} (\boldsymbol{x} - \boldsymbol{x_p}) \times \boldsymbol{e_z} \Gamma_p + \boldsymbol{u_\infty} \qquad (2a)$$

$$\omega_p(\boldsymbol{x}) = \sum_p \zeta_\sigma(|\boldsymbol{x} - \boldsymbol{x}_p|) \Gamma_p \qquad (2b)$$

Here, the Gaussian kernel is used as the smoothing function and so, the participating functions in Equations 2 are:

$$g_\sigma(r) = \frac{1}{2\pi\sigma^2} \left(1 - e^{-\frac{r^2}{2\sigma^2}} \right) \qquad (3a)$$

$$\zeta_\sigma(r) = \frac{1}{2\pi\sigma^2} e^{-\frac{r^2}{2\sigma^2}} \qquad (3b)$$

While VPMs traditionally deal with inviscid flows, advancements have been made to incorporate diffusion effects. By employing Chorin's Viscous Splitting Algorithm [12], the evolution of particles is carried out in two discrete steps:

$$\frac{\partial \omega}{\partial t} + \boldsymbol{u} \cdot \nabla \omega = 0 \qquad \text{convection step} \qquad (4a)$$

$$\frac{\partial \omega}{\partial t} - \nu \nabla^2 \omega = 0 \qquad \text{diffusion step} \qquad (4b)$$

The convection of particles is executed using the 4th order Runge-Kutta method [13], while diffusion is addressed through the implementation of a Vortex Redistribution Method [14]. This method involves redistributing the particles to ensure they do not accumulate in specific regions of the flow due to flow strain. This preventive measure serves to mitigate inaccuracies that might otherwise arise from such accumulations.

2.3. Coupling strategy

The two component solvers are coupled in a two-way fashion, with their coupling occurring only once within a specific time-step. This coupling approach is referred to as weak coupling.

As illustrated in Figure 1, the Eulerian domain is notably narrow compared to typical strategies in Computational Fluid Dynamics (CFD). Consequently, appropriate boundary conditions must be applied. In this context, the vortex particles contribute boundary conditions to the Eulerian boundary by computing the induced velocity field and pressure gradient using the unsteady Bernoulli equation (Eq. 5). This process constitutes the **first coupling step** of the two solvers.

$$\nabla \bar{p} = -(\frac{\partial \boldsymbol{u}}{\partial t} + (\boldsymbol{u} \cdot \nabla)\boldsymbol{u} + \nu\nabla^2\boldsymbol{u}), \qquad \bar{p} = p/\rho \qquad (5)$$

As previously highlighted, Lagrangian solvers often lack accuracy in resolving regions close to boundary layers, rendering their solutions in proximity to solid bodies less reliable. To address this limitation, the Eulerian solution is employed for correction purposes. Particularly, within the interpolation region depicted in Figure 1, the Eulerian solution of the vorticity field is exported and then interpolated onto the vortex particles. This corrective step, constituting the **second coupling step** of the two solvers, enhances the accuracy of the Lagrangian solution in the vicinity of the solid body.

2.4. Handling multibody cases

This solver is adept at handling multi-body simulations in an elegant manner. In particular, as depicted in Figure 2, each cylinder can be treated as an independent OpenFOAM case, solved separately. Particles covering the entire computational domain establish connections between different regions, providing boundary conditions for each separate case. This approach enables the acceleration of simulations by assigning each Eulerian case to a different CPU core.
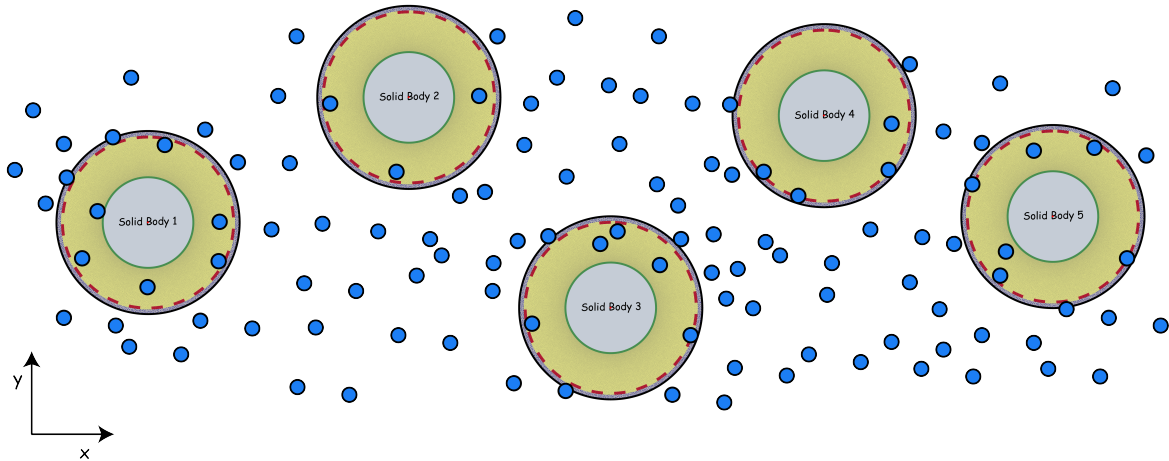

Figure 2: Multi-cylinder problem of independent cylinder cases interconnected by the particles.

3. Validation cases

The validation of the solver will be conducted through a series of tests involving different configurations of two cylinders. Initially, the two cylinders are positioned in tandem arrangement (Figures 3a and 3b). Then, the two cylinders are positioned in staggered arrangement (Figures 3c and 3d). The cases illustrated in Figures 3a and 3c, are both extreme cases, where the Eulerian

meshes of the two cylinders overlap in a large part, which makes these cases very important for the validation of the solver. In all the cases the Reynolds number is set to $Re = 200$. The mesh that is used is comprised solely by hexaedra and it is illustrated in Figure 4. The parameters for the Eulerian solver, the Lagrangian solver and the general simulation parameters are mutual for all the cases, summarized in Table 1.
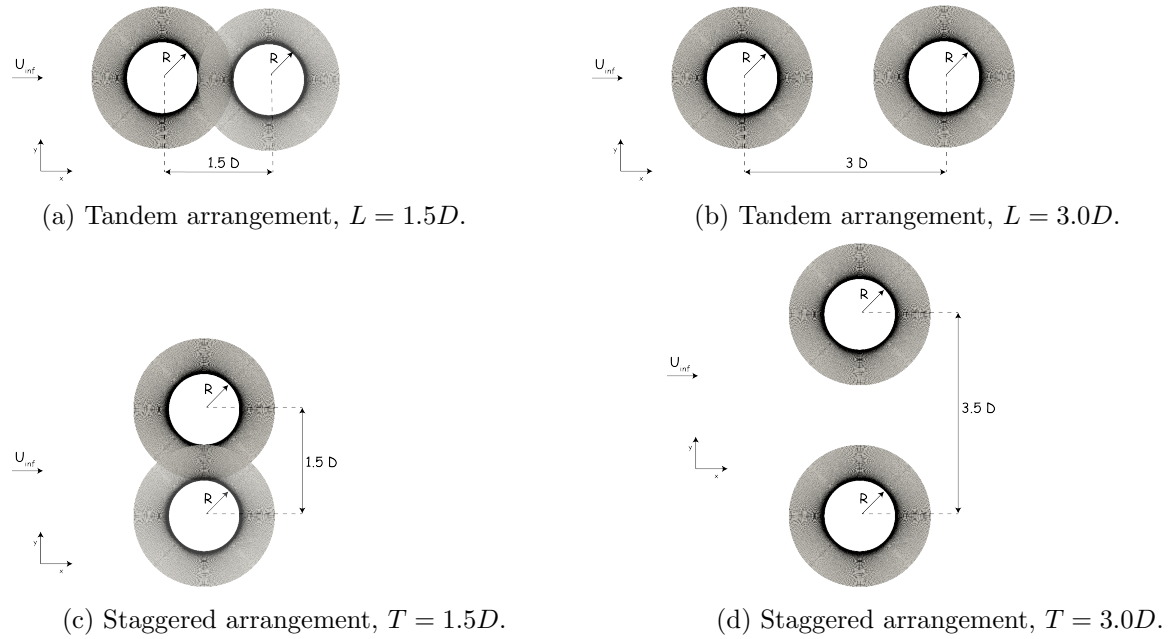

(a) Tandem arrangement, $L = 1.5D$.

(b) Tandem arrangement, $L = 3.0D$.

(c) Staggered arrangement, $T = 1.5D$.

(d) Staggered arrangement, $T = 3.0D$.

Figure 3: The configurations of the validation cases.

Table 1: Global simulation parameters.

Parameter	Symbol	Value	Dimension
Kinematic viscosity	ν	0.005	$kg/(m \cdot s)$
Cylinder's radius	R	0.5	m
Eulerian mesh density	N_{cells}	11040	$-$
Eulerian's domain radius	R_E	1.0	m
Eulerian time-step	Δt_E	0.005	s
Vortex particles spacing	h	0.027	m
Diffusion and convection time step	$\Delta t_c = \Delta t_d$	0.005	s
Interpolation domain offset from Eulerian boundary	d_{bdry}	$3 \cdot h$	m

4. Results and discussion

4.1. Tandem arrangement

For the tandem arrangement of the two cylinders, the results are compared with the corresponding results obtained by Skonecki et al.[15] that used *STAR-CCM+* for their simulations, and by Meneghini et al.[16] where a Finite Element code was used. Table 2 summarizes the results for both cases in tandem arrangement, comparing the mean drag coefficient and the Strouhal number of the current method with the bibliographical results.
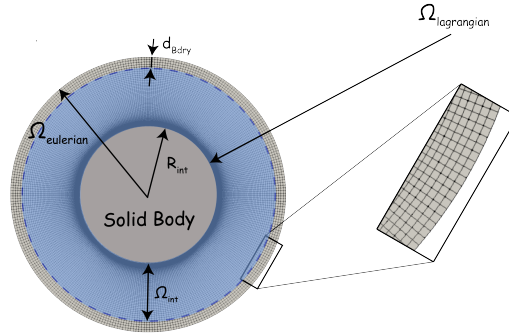
Figure 4: The Eulerian mesh used for the hybrid simulations.

It can be seen that the results of the hybrid solver show a great agreement with the references, for both the front cylinder (denoted with the subscript F) and the rear cylinder (denoted with the subscript R). Figure 5a, illustrates the vorticity field for the two tandem arrangements. It can be observed that the vorticity that is produced in the first cylinder, can accurately be convected to the rear cylinder, and then downstream, without any inaccuracies to be added, neither in the case that the two cylinders are placed very close. Finally, Figure 6a, shows the aerodynamic coefficients over time, for both the front and rear cylinders.

Table 2: Results for tandem arrangement.

Method	**C1** ($L = 1.5D$)				**C2** ($L = 3.0D$)			
	$\overline{C}_{d,F}$	St_F	$\overline{C}_{d,R}$	St_R	$\overline{C}_{d,F}$	St_F	$\overline{C}_{d,R}$	St_R
Skonecki et al.[15]	1.09	0.170	-0.20	0.170	1.02	0.129	-0.12	0.129
Meneghini et al.[16]	1.06	0.167	-0.18	0.167	1.00	0.125	-0.08	0.125
Present Hybrid	1.06	0.167	-0.18	0.167	1.00	0.128	-0.13	0.128

4.2. Staggered arrangement
For the staggered arrangement, the results are compared with the same references. Table 3 summarizes the results for both cases in staggered arrangement, comparing the mean drag coefficient and the Strouhal number of the current method with the bibliographical results. For both the upper cylinder (denoted with the subscript U) and the lower cylinder (denoted with the subscript L), the mean drag coefficient, as well as the Strouhal number, fall between the results obtained from the references. Figure 5a, illustrates the vorticity field, while Figure 6a, shows the aerodynamic coefficients over time, for both the upper and lower cylinders.

Table 3: Results for staggered arrangement.

Method	**C3** ($T = 1.5D$)				**C4** ($T = 3.0D$)			
	$\overline{C}_{d,U}$	St_U	$\overline{C}_{d,L}$	St_L	$\overline{C}_{d,U}$	St_U	$\overline{C}_{d,L}$	St_L
Skonecki et al.[15]	1.55	0.201	1.57	0.204	1.56	0.214	1.56	0.214
Meneghini et al.[16]	1.32	-	1.32	-	1.34	0.174	1.34	0.174
Present Method	1.46	0.209	1.48	0.197	1.41	0.198	1.41	0.198

(a) Tandem arrangement.
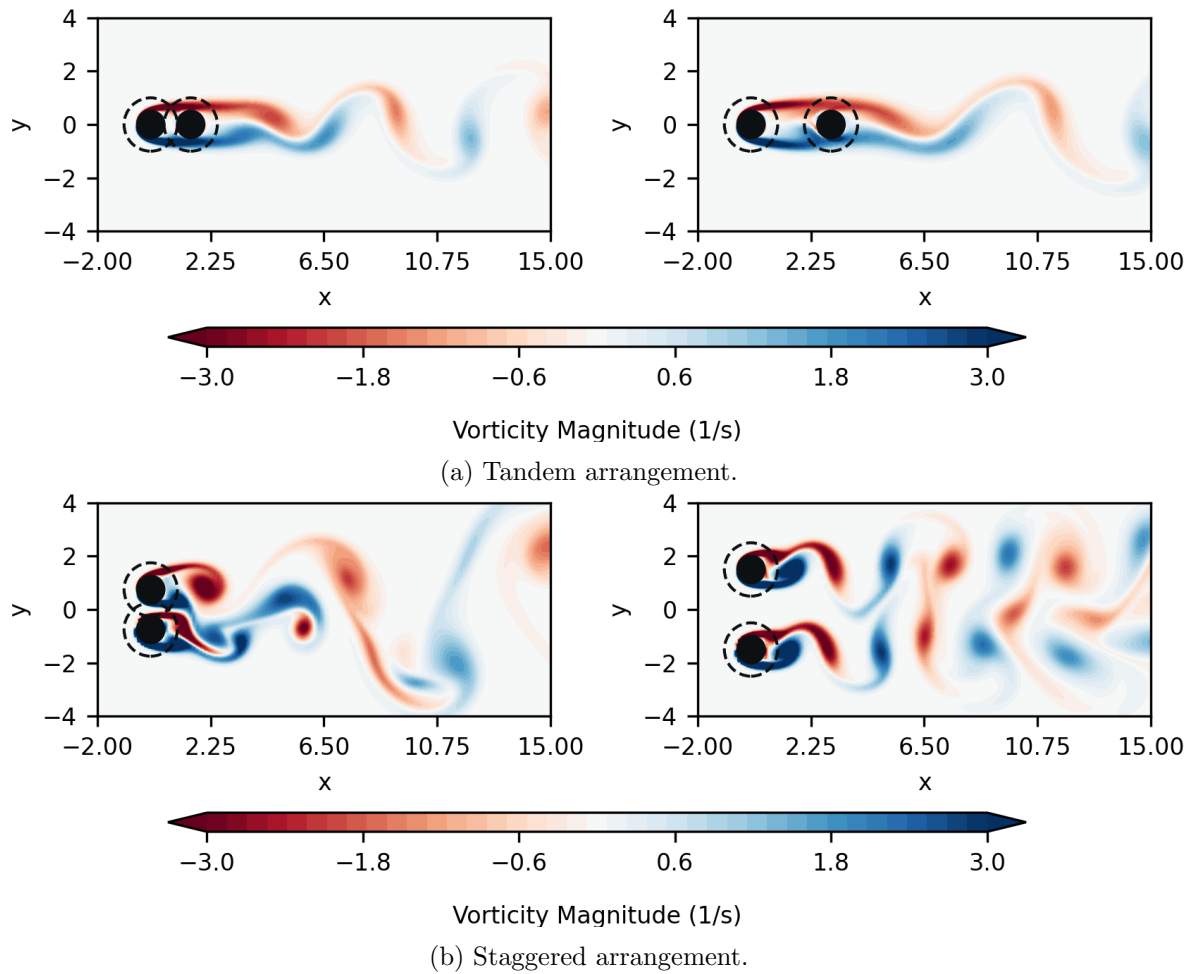

(b) Staggered arrangement.

Figure 5: Screenshots of the vorticity field for the tandem and the staggered arrangements using the hybrid solver.

4.3. Conclusions and Future Aims

The results presented above demonstrate the capability of the proposed hybrid solver to handle multibody problems, producing outcomes consistent with pure Eulerian solvers. Even in cases where the two meshes overlap significantly (such as when the cylinders are placed very close to each other), the results align with existing literature. The versatility of this approach allows for the extension of the problem to incorporate additional cylinders and, subsequently, multiple moving bodies, establishing it as a robust tool in the field of Computational Fluid Dynamics (CFD). While a detailed comparison of the solver's computational efficiency is beyond the scope of this paper, it is worth noting that, given the small number of elements in Eulerian meshes and the utilization of GPUs for particle calculations, the solver demonstrates high efficiency.

It's worth noting that the current solver has also been tested in dynamic mesh simulations [17]. A future goal for the solver is to merge multibody simulations with dynamic mesh simulations. This would enable simulations that approach the complexity of wind farm scenarios, assessing the efficiency and accuracy of the current solver in such cases, which are precisely what it was originally developed for. Moreover, conducting a comparison of the solver's efficiency against conventional Eulerian solvers is necessary. This comparison would be extensive, considering various factors such as time-steps and mesh sizes for both the proposed and conventional solvers,

(a) Aerodynamic coefficients for the tandem arrangement.

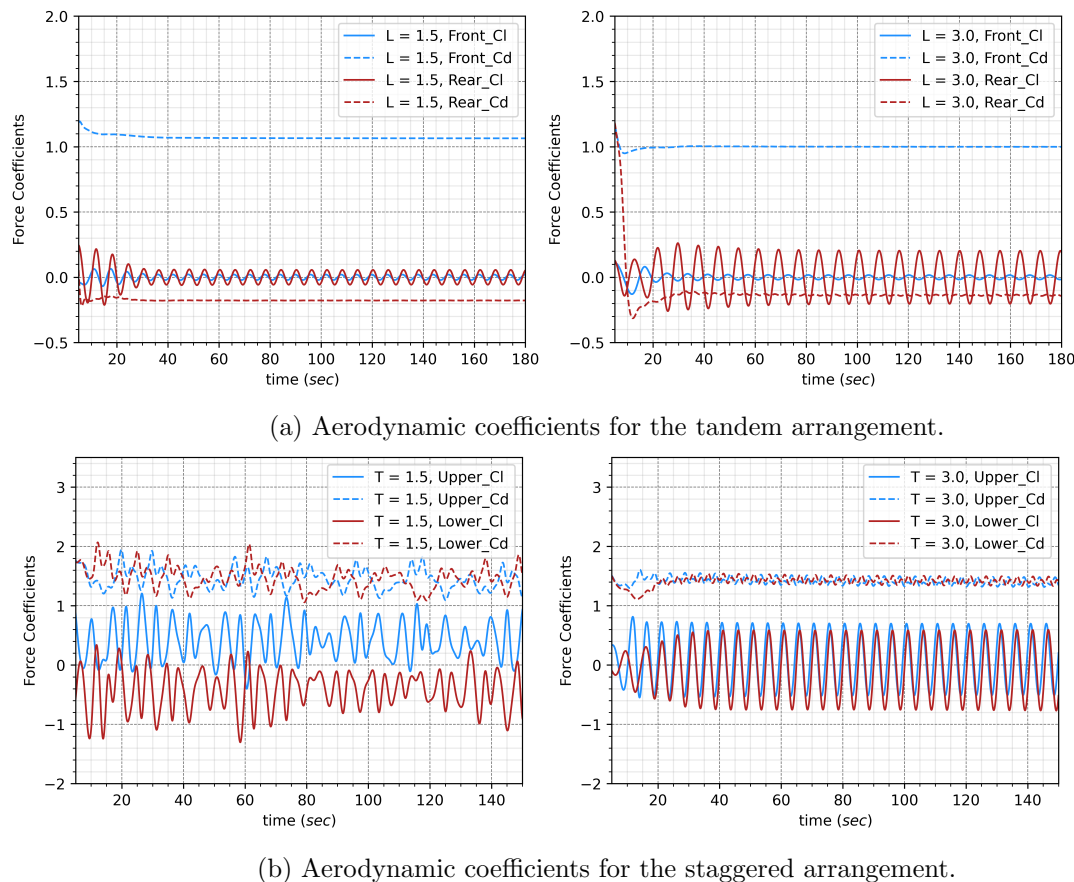(b) Aerodynamic coefficients for the staggered arrangement.

Figure 6: Aerodynamic coefficients for the tandem and the staggered arrangements using the hybrid solver.

the computational domain's length in the conventional solver, and the Lagrangian particles' size and Eulerian subdomain size in the proposed solver, as well as the hardware used in both instances, since conventional CFD can run in parallel on CPUs, while the hybrid approach utilizes GPUs. Taking all these factors into account will allow for a fair comparison between the solvers.

Acknowledgments

References

[1] Maokun Ye and Hamn-Ching Chen and Arjen Koop, Journal of Wind Engineering and Industrial Aerodynamics, Verification and validation of CFD simulations of the NTNU BT1 wind turbine, 2023, 105336, 234

[2] Jessica M.I. Strickland and Richard J.A.M. Stevens, Investigating wind farm blockage in a neutral boundary layer using large-eddy simulations, European Journal of Mechanics - B/Fluids, 303-314 , 95, 2022.

[3] He, Chengjian and Zhao, Jinggen, Modeling Rotor Wake Dynamics with Viscous Vortex Particle Method, AIAA Journal, 47, number=4, 902-915, 2009

[4] Ghazale Kavari, Mojtaba Tahani, Mojtaba Mirhosseini, Wind shear effect on aerodynamic performance and energy production of horizontal axis wind turbines with developing blade element momentum theory, Journal of Cleaner Production, Volume 219, 2019, Pages 368-376, ISSN 0959-6526

[5] Pasolari, R. and Ferreira, C. and van Zuijlen, A., Coupling of OpenFOAM with a Lagrangian vortex particle method for external aerodynamic simulations, Physics of Fluids, Volume 35, 2023, Pages 107115, ISSN 1070-6631

[6] Billuart, P. and Duponcheel, M. and Winckelmans, G. and Chatelain, P., A weak coupling between a near-wall Eulerian solver and a Vortex Particle-Mesh method for the efficient simulation of 2D external flows, Journal of Computational Physics, Volume 473, 2023, Pages 111726, ISSN 0021-9991

[7] Papadakis, George and Voutsinas, Spyros G., A strongly coupled Eulerian Lagrangian method verified in 2D external compressible flows, Computers & Fluids, Volume 195, 2019, Pages 104325, ISSN 0045-7930

[8] Stock, Mark and Gharakhani, Adrin and Stone, Christopher, Modeling Rotor Wakes with a Hybrid OVERFLOW-Vortex Method on a GPU Cluster, 2010, DOI 10.2514/6.2010-4553

[9] Daeninck, Goéric, Developments in hybrid approaches: Vortex method with known separation location; vortex method with near-wall Eulerian solver; RANS-LES coupling, Ph.D. Thesis, Universite Catholique de Louvain, 2006, URL http://hdl.handle.net/2078.1/22806

[10] Palha, A., Manickathan, L., Ferreira, C. S., and Van Bussel, G., A hybrid Eulerian-Lagrangian flow solver, 2015, ArXiv. /abs/1505.03368

[11] OpenFOAM v9, URL https://openfoam.org/version/9/

[12] Chorin A. J., Numerical study of slightly viscous flow, Journal of Fluid Mechanics, Volume 57, 1973, Pages 785–796, DOI 10.1017/S0022112073002016

[13] Runge, C., "Über die numerische Auflösung von Differentialgleichungen," Mathematische Annalen, Volume 46, 1895, Pages 167–178.

[14] Tutty, O. R., A Simple Redistribution Vortex Method (with Accurate Body Forces), 2010, ArXiv. 1009.0166

[15] Skonecki, Gracjan M. and Buick, James M., Numerical Study of Flow around Two Circular Cylinders in Tandem, Side-By-Side and Staggered Arrangements, Fluids, Volume 8, 2023, Pages 148, ISSN 2311-5521

[16] Meneghini, J. R. and Saltara, F. and Siqueira, C. L. R. and Ferrari, J. A., NUMERICAL SIMULATION OF FLOW INTERFERENCE BETWEEN TWO CIRCULAR CYLINDERS IN TANDEM AND SIDE-BY-SIDE ARRANGEMENTS, Journal of Fluids and Structures, Volume 15, 2001, Pages 327–350, ISSN 0889-9746

[17] Pasolari R, Ferreira CS, van Zuijlen A, Baptista CF. Dynamic Mesh Simulations in OpenFOAM: A Hybrid Eulerian–Lagrangian Approach. Fluids. 2024; 9(2):51. https://doi.org/10.3390/fluids9020051

[18] Delft High Performance Computing Centre (DHPC), DelftBlue Supercomputer (Phase 1), URL https://www.tudelft.nl/dhpc/ark:/44463/DelftBluePhase1, 2022